2018 26th Mediterranean Conference on Control and Automation (MED)
Zadar, Croatia, June 19-22, 2018

Attitude and Rate Sensor Bias Estimation for Underwater Vehicles

Erlend K. Jørgensen[1], Ingrid Schjølberg[1]

Abstract— **This paper considers the problem of estimating attitude and rate sensor bias for underwater vehicles, having both proven stability and close-to-optimal performance with respect to noise. Accurate and stable attitude estimates are necessary when performing autonomous underwater operations, and in this paper a novel filter is proposed for estimating attitude and rate sensor bias, using only acoustic and rate sensor measurements. This can provide more robust attitude estimation, as well as enable more accurate accelerometer bias estimation. The suggested filter is proven to be globally exponentially stable except for known singular points, and is based on the eXogenous Kalman Filter principle, in which an estimator with proven stability provides a linearization point for a Linearized Kalman Filter. Experimental validation is provided, and the suggested filter converges and stays close to the true states. The suggested filter is also compared to the conventional Extended Kalman Filter, and a non-implementable Linearized Kalman Filter using the true state as linearization point.**

1. Introduction

Accurate and robust position and attitude estimation is essential for vehicles performing underwater inspection, maintenance and repair (IMR) operations. The most common approach to attitude estimation is the use of two or more reference vectors, known in either the body or the global frame, and measured in the other. These can be used to determine attitude [22]. An algorithm for calculating the rotation matrix explicitly using two non-parallel vector pairs can be found in [5]. For constant reference vectors, a non-linear observer (NLO) for estimating attitude and rate sensor bias with global stability properties was suggested in [12], and extended to time-varying reference vectors in [9], and a GES (under certain assumptions) NLO for attitude is suggested in [10]. It is also common to use the Multiplicative Extended Kalman Filter (MEKF) for attitude estimation [18]. Other approaches for non-linear attitude determination are suggested for example in [20], [3], [4], [17], [21], and a survey can be found in [7].

Traditionally these methods have been applied using the measured acceleration from the accelerometer combined with either magnetometer or gyrocompass measurements. However, these measurements have some weaknesses. The accelerometer is affected by a bias that can cause a bias in the attitude estimate, as well as affected by the vehicle acceleration, as the measurement is usually assumed to be only gravity. The magnetometer is sensitive towards disturbances, from local magnetic fields in the environment, and from the thrusters on the vehicle, whereas the gyrocompass is very accurate, but is heavy, large, expensive and needs to be recalibrated. This paper proposes an estimation scheme that is dependent on neither of these sensors.

A long base-line (LBL) acoustic network is commonly used for accurate positioning of underwater vehicles, and is based on measuring the time-of-arrival (TOA) of an acoustic signal from known, fixed positions on the seabottom. If more receivers are placed on the vehicle, the difference in TOA (DTOA) can also be measured. When the receiver positions are known in the body frame of the vehicle, the DTOA measurements can be used to determine attitude. Such measurements can provide additional ways of estimating attitude, complementing (or replacing) the vector measurements mentioned above. Furthermore, this can enable more accurate accelerometer bias estimation, as estimates of attitude that are independent of the accelerometer measurement is available.

The estimator presented in this paper is based on the general eXogenous Kalman Filter (XKF) principle suggested in [13], in which an estimate with proven stability is used as a linearization point for a Linearized Kalman Filter (LKF). The purpose of this filter structure is to achieve a filter with proven stability, as well as optimal performance wrt. noise provided by the Kalman Filter (KF) framework. This is in contrast to the Extended Kalman Filter (EKF) and particle filter, which have close-to-optimal noise properties, but usually not proven stability, and non-linear observers (NLOs), which have proven stability, but not close-to-optimal noise properties. We use the term close-to-optimal, as there are linearization errors and optimality has not been proven. For more details about particle filters and EKF, see for example [11], and for more details regarding NLOs, see for example [8].

The main contribution of this paper is a suggested filter for estimating attitude and rate sensor bias using only acoustic and rate sensor measurements, along with experimental validation of the proposed filter. The paper builds on the work in [16], in which the attitude is estimated using acoustic, accelerometer and rate sensor measurements. However, for the proposed estimation scheme, accelerometer measurements are avoided. The filter is validated experimentally in MCLab, at the Norwegian University of Science and Technology. The lab consists of a small pool, about $40\,\mathrm{m} \times 6.45\,\mathrm{m} \times 1.5\,\mathrm{m}$ in which ground truth measurements are found from a Qualisys camera positioning system with millimeter accuracy.

The paper is organized as follows. Section 2 describes how to transform the original measurements into the computed measurements. Section 3 shows the overall structure of the

[1]Erlend K. Jørgensen and Ingrid Schjølberg, Department of Marine Technology, University of Science and Technology (NTNU), 7491 Trondheim, Norway

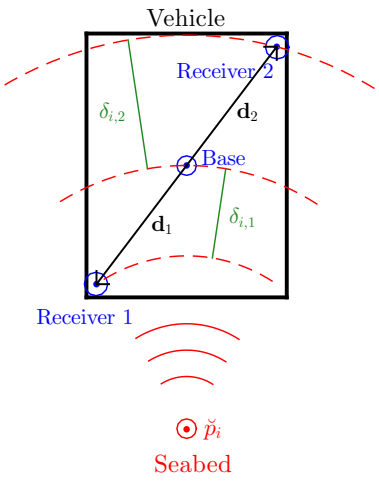

Fig. 1. Illustration of system with pseudo-range-difference measurements. Variables are defined and explained in Sec. 2.2.[16]

filter, and describes each step. Section 4 provides the results, Section 5 gives a short discussion regarding the results, and Section 6 holds the conclusion.

2. Computed Measurements

2.1 Acoustic System Description

The acoustic system applied in this work consists of $N \geq 3$ senders on the seabottom with fixed, known positions in the north-east-down (NED) frame and $M+1 \geq 3$ receivers on the vehicle with fixed, known positions in the body frame. One of the receivers is selected as the base receiver, and M vectors, $\mathbf{d}_{1,..,M}$ are defined, from the base receiver to the remaining receivers. The time difference of arrival between the receivers is measured, and can be used to determine attitude. An illustration of the system is shown in Fig. 1.

2.2 Measurement Models

The two coordinate frames used in modeling are the body frame, and the NED frame, approximated as a local inertial frame with origin defined by the Qualisys system providing ground truth measurements.

A rate sensor is fixed on the ROV and thus follows the body frame, known as a strapdown system. Consequently, the rate sensor measurement, ω^b_{imu}, is modeled as

$$\omega^b_{imu} = \omega^b_{b/n} + \mathbf{b} + \epsilon_\omega \tag{1}$$

where $\omega^b_{b/n}$ is the angular velocity of the body frame wrt. the NED frame, expressed in the body frame, $\mathbf{b}$ is a slowly time-varying rate sensor bias and ϵ_ω is a zero-mean Gaussian white noise vector with covariance $\mathbf{Q}_\omega$.

The model of the pseudo-range-difference measurements is based on the system described in Sec. 2.1. The position of the base receiver is defined as $\mathbf{p}^n = [x, y, z]^T$ and the position of sender i is defined as $\breve{\mathbf{p}}^n_i = [\breve{x}_i, \breve{y}_i, \breve{z}_i]^T$, both in the NED frame. The geometric range is defined as $\rho_i = ct_i = ||\mathbf{p}^n - \breve{\mathbf{p}}^n_i||$ where c is the wave speed, t_i is the TOA from sender i and $||\cdot||$ is the 2-norm. In [23] an acoustic range measurement is given as

$$y_i = \frac{1}{\sqrt{\beta}}(\rho_i + \epsilon_{y,i}) \quad i = 1, .., N \tag{2}$$

where $\epsilon_{y,i}$ is zero-mean Gaussian white noise with variance $\sigma^2_{y,i}$ and β is an unknown, multiplicative parameter to take into account uncertainty in the underwater acoustic wave speed (WS). These are referred to as pseudo-range measurements as they are a function of the geometric range, but also an unknown parameter, β. Based on this formulation, each pseudo-range difference, $\delta_{i,j}$, is modeled as

$$\delta_{i,j} = \frac{1}{\sqrt{\beta}}\left(||\mathbf{p}^n + \mathbf{d}^n_j - \breve{\mathbf{p}}_i{}^n|| - \rho_i + \epsilon_{\delta,i,j}\right), \quad i = 1, .., N,\ j = 1, .., M \tag{3}$$

where $\epsilon_{\delta,i,j}$ is zero-mean Gaussian white noise with variance $\sigma^2_{\delta,i,j}$ and $\mathbf{d}^n_j$ is vector j between receivers, expressed in the NED frame.

Assumption 1. *At least two of the vectors between receivers, $\mathbf{d}^n_j$, are non-parallel for all t, i.e.*

$$\exists\, c \quad s.t. \sum_{i\in\{1,..,M\}} \sum_{j\in\{1,..,M\}\setminus\{i\}} ||\mathbf{d}^n_i \times \mathbf{d}^n_j|| \geq c > 0 \quad \forall\, t$$

Intuitively this makes sense, as determining attitude from vectors requires at least two non-parallel vectors [22], and the suggested filter is based on determining attitude solely by using pesudo-range-difference measurements.

Assumption 2. *The N senders are not colinear*

Calculating the vectors between receivers is based on inverting a matrix containing the sender positions, described in the following section. This matrix will not have full rank, and thus not be invertible if the senders are colinear.

2.3 Calculate Vectors Between Receivers, $\mathbf{d}^n_{1,..,M}$

This section describes how to transform the pseudo-range-difference measurements, $\delta_{i,j}$, into measurements for $\mathbf{d}^n_{1,..,M}$. Based on the pseudo-range-difference measurement model in (3) and that for a vector $\mathbf{v}$, $||\mathbf{v}|| = \sqrt{\mathbf{v}^T\mathbf{v}}$, each pseudo-range difference measurement can be written as [16]

$$\delta_{i,j} = \frac{1}{\sqrt{\beta}}\left(\sqrt{(\Delta\mathbf{p}_i + \mathbf{d}^n_j)^T(\Delta\mathbf{p}_i + \mathbf{d}^n_j)} - \sqrt{(\Delta\mathbf{p}_i)^T(\Delta\mathbf{p}_i)} + \epsilon_{\delta,i,j}\right) \tag{4}$$

where $\Delta\mathbf{p}_i = \mathbf{p}^n - \breve{\mathbf{p}}^n_i = [\Delta x_i, \Delta y_i, \Delta z_i]^T$. Squaring (4), omitting measurement noise for simplicity and performing some algebraic manipulation gives

$$\begin{aligned}(\Delta\mathbf{p}_i + \mathbf{d}^n_j)^T(\Delta\mathbf{p}_i + \mathbf{d}^n_j) = \\ 2(\Delta\mathbf{p}_i)^T\mathbf{d}^n_j + (\Delta\mathbf{p}_i)^T(\Delta\mathbf{p}_i) + ||\mathbf{d}^b_j||^2 = \\ \beta\delta^2_{i,j} + 2\sqrt{\beta}\delta_{i,j}||\Delta\mathbf{p}_i|| + (\Delta\mathbf{p}_i)^T(\Delta\mathbf{p}_i)\end{aligned} \tag{5}$$

By describing $\mathbf{d}^n_j$ as $\mathbf{d}^n_j = [x_{1j}, x_{2j}, x_{3j}] = \mathbf{x}_j$ it is possible to formulate the set of equations given in (5) as

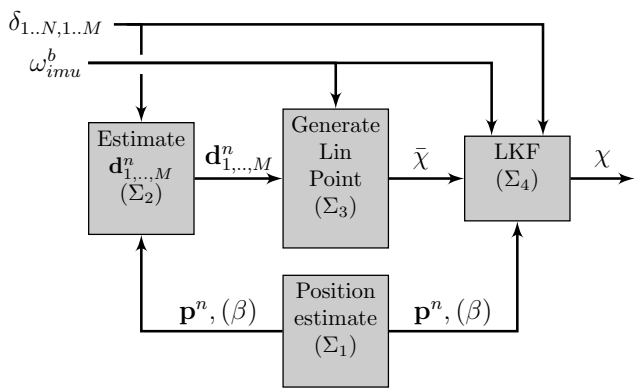

Fig. 2. Filter structure. The output β from the "Position estimate"-block can be set to $\beta = 1$ if it is not available.

a least squares problem with $\mathbf{x}_j$ as the unknown. The set of equations can be written as

$$2(\Delta\mathbf{p}_i)^T\mathbf{x}_j =$$

$$\beta\delta^2_{i,j} + 2\sqrt{\beta}\delta_{i,j}||\Delta\mathbf{p}_i|| - ||\mathbf{d}^b_j||^2 \tag{6}$$

By stacking all measurements, it is possible to write

$$\mathbf{A}\mathbf{x}_j = \mathbf{z}_j \quad j = 1,..,M \tag{7}$$

where

$$\mathbf{A} = \begin{bmatrix} 2(\Delta\mathbf{p}_1)^T \\ \vdots \\ 2(\Delta\mathbf{p}_N)^T \end{bmatrix}$$

$$\mathbf{z}_j = \begin{bmatrix} \beta\delta^2_{1,j} + 2\sqrt{\beta}\delta_{1,j}||\Delta\mathbf{p}_1|| - ||\mathbf{d}^b_j||^2 \\ \vdots \\ \beta\delta^2_{N,j} + 2\sqrt{\beta}\delta_{N,j}||\Delta\mathbf{p}_N|| - ||\mathbf{d}^b_j||^2 \end{bmatrix}$$

If assumption 2 is fulfilled, $\mathbf{A}$ will have full rank, and it is possible to solve (7) as a least squares problem, thus making measurements for $\mathbf{d}^n_{1,..,M}$ available.

3. Attitude and Rate Sensor Bias Filter

As mentioned in Sec. 1, the suggested filter is based on the XKF principle, in which an auxiliary estimator with proven stability is used to generate a linearization point for a LKF. The principle is based on avoiding feedback loops in the estimator, simplifying stability analysis significantly. This is in contrast to the EKF in which the linearization point is the filter's own estimate, resulting in a feedback loop that can cause instability. If the linearization of the model used in the LKF in Σ_4 is uniformly completely observable (UCO) and uniformly completely controllable (UCC), and the system satistfies criteria stated in [13], the LKF inherits the stability properties of the auxiliary estimator. The overall structure of the filter is shown in Fig. 2.

3.1 Subsystem Σ_1: Position Estimate

Subsystem Σ_1 provides a position estimate and, if available, an estimate of β (otherwise set to $\beta = 1$). Any filter that is proven to be globally exponentially stable (GES), taking pseudo-range measurements (and possibly depth measurements) as input can be used for this purpose. The filter used in the experiment is suggested in [15], and is also based on the XKF principle.

The position estimate filter in Σ_1 is also responsible for performing outlier detection for the range measurements. Outliers occured during testing, and a simple outlier detection scheme based on the Mahalanobis distance [2] seemed sufficient.

3.2 Subsystem Σ_2: Estimate Vectors Between Receivers, $\mathbf{d}^n_{1,..,M}$

This subsystem performs the calculation of $\mathbf{d}^n_{1,..,M}$ from TDOA measurements and the estimates for $\mathbf{p}^n$ and β. However, as the measurements are constructed by performing a non-linear transform of noisy measurements, the measurements for $\mathbf{d}^n_{1,..,M}$ are noisy. Consequently, a KF is used for filtering these measurements to provide more stable estimates of $\mathbf{d}^n_{1,..,M}$.

The calculated $\mathbf{d}^n_{1,..,M}$ as described in Sec. 2.3 is used as input for a Kalman filter with model given by

$$\begin{aligned} \dot{\mathbf{d}}^n_j &= \mathbf{a}^n_j \\ \dot{\mathbf{a}}^n_j &= \epsilon_d \\ \mathbf{y}_d &= \mathbf{d}^n_j + \epsilon_y \end{aligned} \tag{8}$$

where ϵ_d and ϵ_y are zero-mean Gaussian white noise vectors and $\mathbf{y}_d$ is the calculated measurement of $\mathbf{d}^n_j$. The covariance matrix of ϵ_d, $\mathbf{Q}_d$ is tuned based on expected rate of change in attitude for the vehicle and the covariance matrix of ϵ_y can be calculated from the finite differences approach, combined with the values of $\sigma^2_{\delta,i,j}$.

3.3 Subsystem Σ_3: Generate Linearization Point

The purpose of subsystem Σ_3 is to estimate attitude and rate sensor bias to be used as a linearization point for the LKF in Σ_4. The estimator should take two or more vector measurements as input along with rate sensor measurements, and the output should be attitude and rate sensor bias. Furthermore, the estimator should have proven stability, preferrably GES, or something close to GES.

Any NLO that satisfies these criteria can be applied. The NLO used in this paper is suggested in [10], which provides an estimate of the attitude described by a $3\,x\,3$ matrix asymptotically converging towards a rotational matrix, and the rate sensor bias. This NLO is GES if Assumption 1 is fulfilled, along with a known upper bound for the bias, a design property regarding the matrices used in the estimator is fulfilled, and one of the tuning parameters is above a lower bound. For more details about the estimator and its use in the filter, see [16].

The output from the chosen NLO is a rotation matrix and rate sensor bias. As the states chosen for the filter are Euler

angles and rate sensor bias, the rotation matrix is converted into Euler angles before it is given as output. The total output of the NLO is the Euler angles linearization point, $\bar{\mathbf{\Theta}}$ and the rate sensor bias linearization point, $\bar{\mathbf{b}}$, combined in the vector $\bar{\chi} = \begin{bmatrix} \bar{\mathbf{\Theta}}^T & \bar{\mathbf{b}}^T \end{bmatrix}^T$.

3.4 Subsystem Σ_4: Linearized Kalman Filter

The LKF is based on linearizing the system model about the linearization point from Σ_3, $\bar{\chi}$. The chosen attitude representation is Euler angles, and more specifically the roll-pitch-yaw convention, $\mathbf{R}_b^n(\mathbf{\Theta}) = \mathbf{R}_z(\psi)\mathbf{R}_y(\theta)\mathbf{R}_x(\phi)$. The system is modelled as

$$\dot{\chi} = \begin{bmatrix} \mathbf{T}(\chi)(\omega_{imu}^b - \mathbf{b} - \epsilon_\omega) \\ \epsilon_b \end{bmatrix} \tag{9}$$

where $\epsilon_\chi = [\epsilon_\omega^T, \epsilon_b^T]^T$ is a vector of two zero-mean Gaussian white noise vectors with covariances $\mathbf{Q}_\omega$ and $\mathbf{Q}_b$ and $\mathbf{T}$ is derived in [8], given by

$$\mathbf{T} = \begin{bmatrix} 1 & s\phi t\theta & c\phi t\theta \\ 0 & c\phi & -s\phi \\ 0 & s\phi/c\theta & c\phi/c\theta \end{bmatrix} \tag{10}$$

where $s\cdot = \sin(\cdot)$, $c\cdot = \cos(\cdot)$ and $t\cdot = \tan(\cdot)$, and $\chi = [\mathbf{\Theta}^T, \mathbf{b}^T]^T$. The measurement equation is given by

$$\mathbf{y}_{LKF} = \mathbf{h}(\chi) = \begin{bmatrix} \delta_{1,1} \\ \vdots \\ \delta_{N,M} \end{bmatrix} + \epsilon_h \tag{11}$$

where ϵ_h is a vector of zero-mean Gaussian white noise with covariance $\mathbf{R}_h$. As both the dynamic model and the measurement model are non-linear with respect to the state, both of these models have to be linearized to be used in a KF. The chosen linearization scheme is the first order Taylor approximation, given by

$$\mathbf{f}(\mathbf{v}) \approx \mathbf{f}(\bar{\mathbf{v}}) + \left.\frac{\mathrm{d}\mathbf{f}(\mathbf{v})}{\mathrm{d}\mathbf{v}}\right|_{\mathbf{v}=\bar{\mathbf{v}}} (\mathbf{v} - \bar{\mathbf{v}}) \tag{12}$$

where $\mathbf{f}$ is a vector function, $\mathbf{v}$ is a vector and $\bar{\mathbf{v}}$ is the linearization point. Furthermore, the first order Euler discretization is used as a discretization scheme.

As can be seen in (10), the filter has singularities at $\theta = \pi/2 + k\pi$, $k \in \mathbb{Z}$ in the dynamic model. This is a well known problem with using Euler angles. However, the singularities are well known, and it is possible to switch to a representation with different singularities if necessary [8]. Furthermore, as the normal state for most underwater vehicles is $\phi \approx 0$ and $\theta \approx 0$, the singularities will rarely occur for most conventional underwater vehicles.

3.5 Stability Analysis

An analysis of the stability of a cascade structure in which estimates from a GES estimator are used as parameters in a KF instead of the true values can be found in [14], and the system is proven to be GES. Thus, using the estimates from Σ_1 instead of the true values for $\mathbf{p}^n$ and β does not affect stability.

As mentioned in Sec. 3.3, the NLO chosen is GES under certain assumptions and criteria. Consequently, as described in [13], if the linearization of the model in the LKF in Σ_4 is UCO and UCC, the LKF in Σ_4 will inherit the stability properties of the estimator in Σ_3 (in this case, GES).

It is shown in Sec. 2.3 how to transform, with a known position and β, $[\delta_{1,1} \cdots \delta_{N,M}]^T$ into two or more vectors in the NED frame. Two or more non-parallel vectors known in the body frame and measured in the NED frame can be used to fully determine attitude [22]. Consequently, if Assumption 1 and 2 is fulfilled, $[\delta_{1,1} \cdots \delta_{N,M}]^T$ can be simplified as a full attitude measurement. The simplified measurement model can now be written as

$$\mathbf{h}(\chi) = \mathbf{\Theta} \tag{13}$$

For stability analysis, the model is linearized around the exogenous linearization point $\bar{\chi}$

$$\dot{\chi} = \mathbf{f}(\chi) = \mathbf{f}(\bar{\chi}) + \mathbf{F}(t)(\chi - \bar{\chi}) + \mathbf{G}(t)\epsilon_\chi + \gamma_\chi(t) \tag{14}$$

$$\mathbf{h}(\chi) = \mathbf{h}(\bar{\chi}) + \mathbf{H}(t)(\chi - \bar{\chi}) + \epsilon_h + \gamma_h(t) \tag{15}$$

where $\gamma_\chi(t)$ and $\gamma_h(t)$ are the linearization errors. For the current stability analysis it is not necessary to know $\mathbf{F}(t)$, $\mathbf{G}(t)$ and $\mathbf{H}(t)$ fully. However, the structure of the matrices is important, and some parts of the matrices are needed explicitly to prove stability. We define $\mathbf{I}_i$ as a $i\,x\,i$ identity matrix and $\mathbf{0}_i$ as a $i\,x\,i$ matrix of zeros. It is possible to write

$$\mathbf{F}(t) = \left.\frac{\mathrm{d}\mathbf{f}(\chi)}{\mathrm{d}\chi}\right|_{\chi=\bar{\chi}} = \begin{bmatrix} \mathbf{A}_1 & -\mathbf{T} \\ \mathbf{0}_3 & \mathbf{0}_3 \end{bmatrix} \tag{16}$$

$$\mathbf{G}(t) = \left.\frac{\mathrm{d}\mathbf{f}(\chi)}{\mathrm{d}\epsilon_\chi}\right|_{\chi=\bar{\chi}} = \begin{bmatrix} -\mathbf{T} & \mathbf{0}_3 \\ \mathbf{0}_3 & \mathbf{I}_3 \end{bmatrix} \tag{17}$$

$$\mathbf{H}(t) = \left.\frac{\mathrm{d}\mathbf{h}(\chi)}{\mathrm{d}\chi}\right|_{\chi=\bar{\chi}} = \begin{bmatrix} \mathbf{I}_3 & \mathbf{0}_3 \end{bmatrix} \tag{18}$$

where $\mathbf{A}_1$ is an unknown matrix, $\mathbf{T}$ is defined in (10). It is stated in [13] that for the XKF to inherit stability properties of the NLO providing the linearization point, the model in the LKF must be uniformly completely observable (UCO) and uniformly completely controllable (UCC).

It is stated in [6] that the pair $(\mathbf{F}(t), \mathbf{H}(t))$ is UCO if the observability co-distribution given by

$$\mathrm{d}\mathcal{O} = \begin{bmatrix} M_0(t, \hat{\chi}) \\ \vdots \\ M_{n-1}(t, \hat{\chi}) \end{bmatrix} \tag{19}$$

has full rank for all t, where

$$M_0(t, \hat{\chi}) = \mathbf{H}(t)$$

$$M_m(t, \hat{\chi}) = M_{m-1}(t, \hat{\chi})\mathbf{F}(t) + \frac{\mathrm{d}}{\mathrm{d}t} M_{m-1}(t, \hat{\chi})$$

for $m = 0, ..., n-1$ where n is the state space dimension. If the observability co-distribution for $m = 0, 1$ has full rank, the full observability co-distribution will also have full rank. It can be found from [19] that for the matrix

$$\mathrm{d}\mathcal{O} = \begin{bmatrix} M_0(t, \hat{\chi}) \\ M_1(t, \hat{\chi}) \end{bmatrix} = \begin{bmatrix} \mathcal{O}_1 & \mathbf{0}_3 \\ \mathcal{O}_2 & \mathcal{O}_3 \end{bmatrix}$$

TABLE I

SENDER POSITIONS AND VECTORS BETWEEN RECEIVERS

Parameter	$\breve{\mathbf{p}}_1^n$	$\breve{\mathbf{p}}_2^n$	$\breve{\mathbf{p}}_3^n$	$\breve{\mathbf{p}}_4^n$
x[m]	-0.469	4.74	4.33	-0.429
y[m]	1.92	1.13	-2.01	-2.09
z[m]	-0.697	-0.169	-0.701	-0.116
Parameter	$\mathbf{d}_1^b$	$\mathbf{d}_2^b$		
x[m]	0.40	-0.82		
y[m]	-0.57	-0.58		
z[m]	-0.80	-0.77		

$\text{rank}(\text{d}\mathcal{O}) \geq \text{rank}(\mathcal{O}_1) + \text{rank}(\mathcal{O}_3)$.

$\mathcal{O}_1$ is defined as $\mathbf{I}_3$ in (18), and $\mathcal{O}_3$ is given by $\mathcal{O}_3 = -\mathbf{T}$. We define $\Pi = \{\pi/2 + k\pi : k \in \mathbb{Z}\}$. As $\mathbf{T}(\bar{\chi})$ is created from inverting $\mathbf{T}^{-1}(\bar{\chi})$, $\mathbf{T}(\bar{\chi})$ will be non-singular and have full rank for $\theta \notin \Pi$. Consequently, if $\text{rank}(\mathcal{O}_1) = 3$ and $\text{rank}(\mathcal{O}_3) = 3$ for $\theta \notin \Pi$, $\text{rank}(\text{d}\mathcal{O}) = 6$ for $\theta \notin \Pi$ proving the system is UCO for $\theta \notin \Pi$.

It is stated in [6] that the pair $(\mathbf{F}(t), \mathbf{G}(t))$ is UCC if the controllability co-distribution given by

$$\text{d}\mathcal{C} = \begin{bmatrix} M_0(t,\hat{\chi}) & \cdots & M_{n-1}(t,\hat{\chi}) \end{bmatrix} \tag{20}$$

has full rank for all t, where

$$M_0(t,\hat{\chi}) = \mathbf{G}(t)$$

$$M_m(t,\hat{\chi}) = \mathbf{F}_x(t) M_{m-1}(t,\hat{\chi}) + \frac{\text{d}}{\text{d}t} M_{m-1}(t,\hat{\chi})$$

for $m = 0, ..., n-1$ where n is the state space dimension. As $\text{rank}(\mathbf{G}(t)) = 6$ for $\theta \notin \Pi$, the system is UCC for $\theta \notin \Pi$.

As can be seen from the stability analysis, the system is GES except for the singularities given by $\theta \in \Pi$. This is a minor problem in practice, as the singularities are known, and it is possible to switch between representations.

4. TESTING AND RESULTS

4.1 System Setup

The proposed filter was implemented and tested in a wet laboratory pool. A square aluminium frame was built to represent the underwater vehicle and three acoustic receivers were placed on the frame, as shown in Fig. 3. Four transponders were located on the bottom of the pool in a rectangular pattern. The acoustic system was provided by Water Linked [1] and the acoustic measurements have a frequency of 1 Hz. The values for the sender positions and $\mathbf{d}_{1,2}^b$ are given in Tab. I. The pool system has an underwater localization system provided by Qualisys, which supplies the ground truth for the aluminium frame (vehicle) during the experiment. Ground truth position and attitude is shown in Fig. 4. The rate sensor used is from an ADIS16485, a microelectromechanical IMU with a price of around $1,600. The IMU data is read with a frequency of 100 Hz.

The tuning parameter values for Σ_2 and Σ_4 can be seen in Tab II and Tab III, subsequently. $\mathbf{P}_0$ is the initial

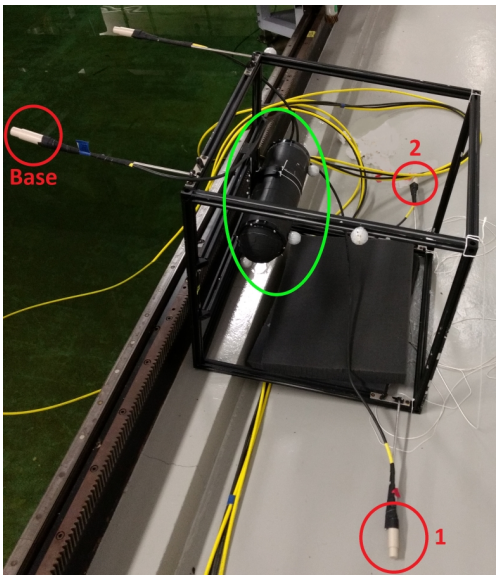

Fig. 3. Aluminum frame representing the vehicle with receiver setup. In the image the frame is tilted sideways. Base receiver, receiver 1 and receiver 2 are marked with red circles. and the tube containing the IMU is within the green ellipse

TABLE II

TUNING PARAMETER VALUES FOR Σ_2

Parameter	$\mathbf{Q}_d$	$\sigma^2_{\delta,i,j}$
Value	$3^2 \cdot \mathbf{I}_3$	0.2^2
Parameter	$\mathbf{x}_0$	$\mathbf{P}_0$
Value	$\mathbf{0}_{6x1}$	$\text{diag}(\mathbf{0.5}^2_{6x1})$

covariance matrix for the KFs, $\mathbf{x}_0$ is the initial estimate for each subsystem and $\mathbf{k}_{i\,x\,j}$ means an i times j matrix with containing the value $\mathbf{k}$. $\text{diag}(\mathbf{v})$ is a diagonal matrix with the vector $\mathbf{v}$ along the diagonal.

For comparison, an EKF is also run, with the same tuning as the LKF in Σ_4, using the filter's own state as the linearization point, denoted χ_{EKF}. Furthermore, a LKF using the true state as linearization point is also run. This filter is impossible to implement in a real scenario, as it requires knowing the true state, but is valuable for comparison, as can be viewed as the optimal performance for the given scenario. The optimal LKF is denoted χ_{opt}.

4.2 Results

The raw acoustic pseudo-range measurements can be seen in Fig. 5. The first pseudo-range measurements occur at $t \approx 2.8\,\text{s}$, and throughout the experiment around $0.2\,\%$ of the pseudo-range measurements were rejected as outliers. The linearization point from Σ_3 is denoted as $\bar{\chi}$. The Euler angle errors are shown in Fig. 6. As there is no ground truth for rate sensor bias, the estimates are shown and not the estimate errors. However, the end estimate for rate sensor bias is $\mathbf{b}_\chi = [-3.7, 2.7, 3.0] \cdot 10^{-3}$ whereas the bias was found in calibration to be $\mathbf{b}_{cal} = [-3.7, 2.8, 3.2] \cdot 10^{-3}$,

TABLE III

TUNING PARAMETER VALUES FOR Σ_4

Parameter	$\mathbf{Q}_\omega$	$\mathbf{Q}_b$	$\mathbf{R}_h$
Value	$0.05^2 \cdot \mathbf{I}_3$	$\left(1 \cdot 10^{-4}\right)^2 \cdot \mathbf{I}_3$	$\mathrm{diag}([\mathbf{0.2}^2_{8x1}])$

Parameter	$\mathbf{x}_0$	$\mathbf{P}_0$
Value	$\begin{bmatrix} 1 \\ 1 \\ 0 \\ \mathbf{0}_{3x1} \end{bmatrix}$	$\mathrm{diag}(\begin{bmatrix} \mathbf{2}^2_{3x1} \\ \mathbf{0.1}_{3x1} \end{bmatrix})$

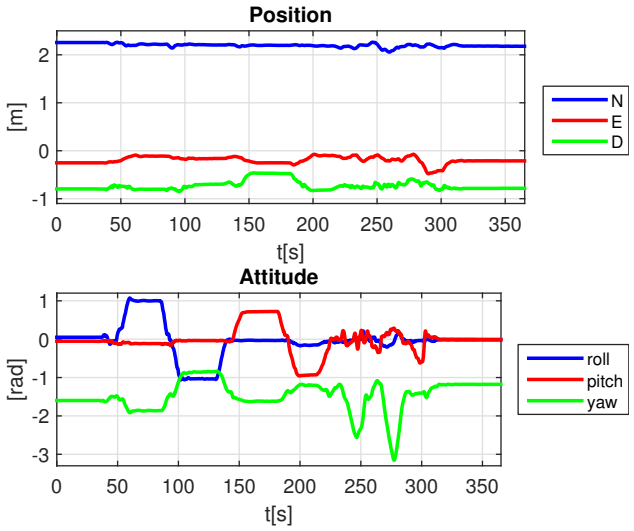

Fig. 4. Ground truth position and Euler angles from the Qualisys system

which is very similar considering noise levels in the system and uncertainty in calibration. Rate sensor bias estimates are shown in Fig. 7.

It is clear that the linearization point, $\bar{\chi}$, is less accurate than the output from the suggested filter, χ. This supports the claim that using the output from the estimator with proven stability as a linearization point for a LKF increases accuracy of the filter (while preserving stability properties). It can also be seen that the EKF takes longer to converge than the suggested filter, and also has less accurate stationary performance.

The suggested filter converges, and performs very similarly to the optimal LKF in both the transient and the stationary state. The RMSE's after convergence for all filters are shown in Tab IV. The suggested filter has similar RMSE as the optimal filter, although slightly larger for roll angle. The RMSE for the pitch angle of the EKF is said to be not applicable, as it is viewed to not converge before the end of the experiment (see Fig. 6 for details).

5. DISCUSSION

The tuning of Kalman Filters was based on approximating the measurement noise for each of the measurements when the vehicle was stationary, and the expected rate of change in

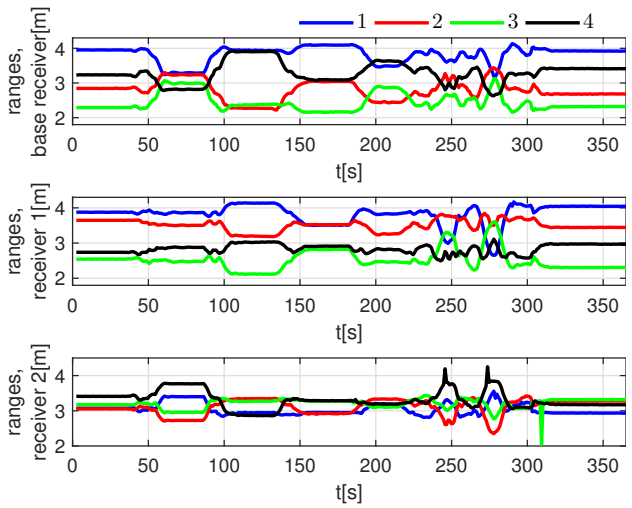

Fig. 5. Raw measured acoustic pseudo-ranges for all three receivers. Pseudo-range i is the range measured from the sender at $\check{\mathbf{p}}^n_i$.

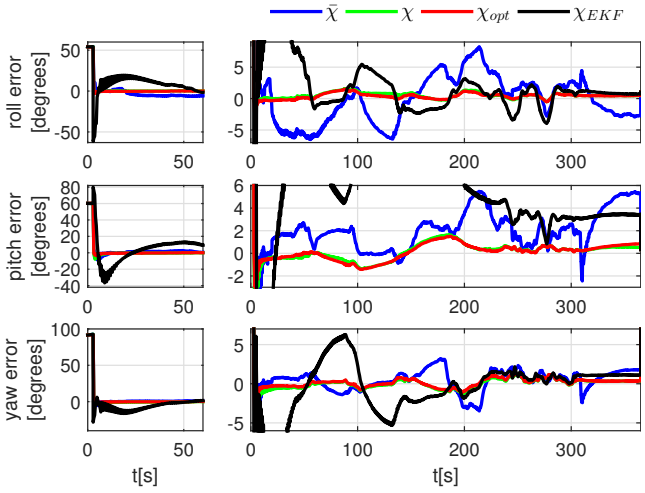

Fig. 6. Euler angle estimation errors. Two axis are chosen to show both transient and stationary behaviour

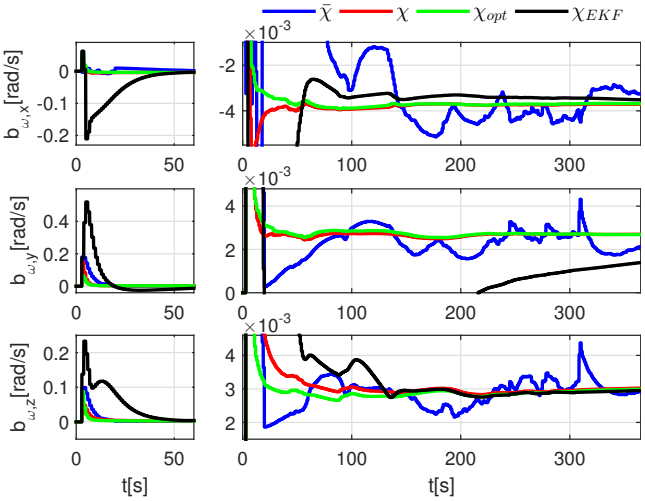

Fig. 7. Estimated rate sensor bias. Two axis are chosen to show both transient and stationary behaviour

TABLE IV

RMSE FOR [ROLL ANGLE, PITCH ANGLE, YAW ANGLE] AFTER CONVERGENCE FOR ALL FILTERS.

RMSE[degrees]	$\bar{\chi}$	$[3.2, 2.7, 1.4]$
	χ	$[0.71, 0.72, 0.65]$
	χ_{opt}	$[0.66, 0.71, 0.66]$
	χ_{EKF}	$[2.4, \mathrm{n/a}, 2.4]$

the system. However, as the NLO chosen in Σ_3 is derived to achieve mathematical stability, the parameters for tuning Σ_3 are not as intuitive. Consequently, these tuning parameters were chosen through a process of trial and error, and a different tuning might have given more accurate results.

A different tuning of the EKF could also have resulted in more accurate performance. However, the tuning chosen is based on realistic values, and a different tuning through trial and error would result in something that might work well for the specific experiment, but have unpredictable behaviour in general.

It is important to note that the term "optimal" when used in this paper is wrt. the given scenario. The performance of the filter is dependent on sender position, receiver position, measurement noise and the rate of change in the system states. Especially placement of senders and receivers affect the geometric properties of the system, and more specifically the conditioning of the matrix $\mathbf{A}$ in (7), and it is desirable (although not necessary) to have large differences in x, y and z values for the senders. Consequently, these aspects must be considered when placing senders and receivers during system design. For further discussion, see [14].

6. CONCLUSIONS

Attitude and position estimation are central parts of autonomous underwater inspection, maintenance and repair (IMR) operations. A filter estimating attitude and rate sensor bias using acoustic and rate sensor measurements has been suggested. This can provide more robust attitude estimation, and can also enable more accurate accelerometer bias estimation, as an attitude measurement that is decoupled from the accelerometer measurement is available. The filter is based on the XKF principle, in which an estimator with proven stability is used to provide an exogenous linearization point for a LKF, yielding both proven stability and close-to-optimal noise properties for bounded noise. The filter is proven to be GES except for two known singular points, in contrast to the EKF which does not have proven stability for the given model.

Experimental validation has been provided. The filter converges, and stays close to the ground truth values throughout the experiment. A non-implementable optimal filter using the true state as linearization point is run for comparison, and both transient and stationary performance of the suggested filter is similar.

7. ACKNOWLEDGEMENTS

This work is supported by the NTNU Center of Autonomous Marine Operations and Systems (NTNU AMOS), grant no. 223254 and NextGenIMR, grant no. 234108.

REFERENCES

[1] Waterlinked webpage. https://waterlinked.com/. Accessed: 2017-07-01.

[2] Yaakov Bar-Shalom. *Tracking and data association*. Academic Press Professional, Inc., 1987.

[3] Pedro Batista, Carlos Silvestre, and Paulo Oliveira. Ges integrated lbl/usbl navigation system for underwater vehicles. In *Decision and Control (CDC), 2012 IEEE 51st Annual Conference on*, pages 6609–6614. IEEE, 2012.

[4] Pedro Batista, Carlos Silvestre, and Paulo Oliveira. Globally exponentially stable cascade observers for attitude estimation. *Control Engineering Practice*, 20(2):148–155, 2012.

[5] Harold D Black. A passive system for determining the attitude of a satellite. *AIAA journal*, 2(7):1350–1351, 1964.

[6] Chi-Tsong Chen. *Linear system theory and design*. Oxford University Press, Inc., 1995.

[7] John L Crassidis, F Landis Markley, and Yang Cheng. Survey of nonlinear attitude estimation methods. *Journal of guidance, control, and dynamics*, 30(1):12–28, 2007.

[8] Thor I Fossen. *Handbook of marine craft hydrodynamics and motion control*. John Wiley & Sons, 2011.

[9] Håvard Fjær Grip, Thor I Fossen, Tor A Johansen, and Ali Saberi. Attitude estimation using biased gyro and vector measurements with time-varying reference vectors. *IEEE Transactions on Automatic Control*, 57(5):1332–1338, 2012.

[10] Håvard Fjær Grip, Thor I Fossen, Tor A Johansen, and Ali Saberi. Globally exponentially stable attitude and gyro bias estimation with application to gnss/ins integration. *Automatica*, 51:158–166, 2015.

[11] Fredrik Gustafsson. *Statistical sensor fusion*. Studentlitteratur,, 2010.

[12] Tarek Hamel and Robert Mahony. Attitude estimation on so [3] based on direct inertial measurements. In *Proceedings 2006 IEEE International Conference on Robotics and Automation, 2006. ICRA 2006.*, pages 2170–2175. IEEE, 2006.

[13] Tor A Johansen and Thor I Fossen. The exogenous kalman filter (xkf). *International Journal of Control*, 90(2):161–167, 2017.

[14] Erlend K Jørgensen. *Navigation and Control of Underwater Robotic Vehicles*. PhD thesis, Norwegian University of Science and Technology, 2018.

[15] Erlend K Jørgensen, Tor A Johansen, and Ingrid Schjølberg. Enhanced hydroacoustic range robustness of three-stage position filter based on long baseline measurements with unknown wave speed. *IFAC-PapersOnLine*, 49(23):61–67, 2016.

[16] Erlend K Jørgensen and Ingrid Schjølberg. Attitude and gyro bias estimation using range-difference and imu measurements. In *Autonomous Underwater Vehicles (AUV), 2016 IEEE/OES*, pages 124–130. IEEE, 2016.

[17] Robert Mahony, Tarek Hamel, and Jean-Michel Pflimlin. Nonlinear complementary filters on the special orthogonal group. *IEEE Transactions on automatic control*, 53(5):1203–1218, 2008.

[18] F Landis Markley et al. Attitude error representations for kalman filtering. *Journal of guidance control and dynamics*, 26(2):311–317, 2003.

[19] Carl D Meyer, Jr. Generalized inverses and ranks of block matrices. *SIAM Journal on Applied Mathematics*, 25(4):597–602, 1973.

[20] Angelo M Sabatini. Quaternion-based extended kalman filter for determining orientation by inertial and magnetic sensing. *IEEE Transactions on Biomedical Engineering*, 53(7):1346–1356, 2006.

[21] S Salcudean. A globally convergent angular velocity observer for rigid body motion. *IEEE transactions on Automatic Control*, 36(12):1493–1497, 1991.

[22] Malcolm David Shuster and S. D. Oh. Three-axis attitude determination from vector observations. *Journal of Guidance, Control, and Dynamics*, 2012.

[23] Bård B Stovner, Tor A Johansen, Thor I Fossen, and Ingrid Schjølberg. Three-stage filter for position and velocity estimation from long baseline measurements with unknown wave speed. In *American Control Conference (ACC), 2016*, pages 4532–4538. IEEE, 2016.